

Hydrothermal synthesis of struvite and its phase transition: Impacts of pH, heating and subsequent cooling methods



A.P. Bayuseno^{a,*}, W.W. Schmahl^b

^a Center for Waste Management, Mechanical Engineering Graduate Program, Diponegoro University, Tembalang Campus, Semarang, Indonesia

^b Department of Earth-and Environmental Sciences, Ludwig-Maximilian- University of Munich , Germany

ARTICLE INFO

Communicated by Gen Sazaki

Keywords:

A2. MAP precipitation
A2. Hydrothermal synthesis
A2. Phosphate recovery
B1. Struvite
B1. Dittmarite

ABSTRACT

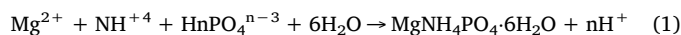
MAP (magnesium, ammonium, and phosphate) precipitation under hydrothermal condition was investigated in the present study. The hydrothermal mediated solution of a MAP in equimolar ratios (1:1:1) was prepared for crystal growth in a reactor autoclave. In the hydrothermal experiments, the reactor was heated in a furnace at varying temperatures (60, 80 and 120 °C) for 24 h, and then followed by (i) air cooling and (ii) water quenching to room temperature. Struvite could be formed in the solution with initial pH values (7–10) when the reactor worked at 60 °C for 24 h and was subsequently air-cooled and water-quenched to room temperature. Working with the temperature of 80 °C and subsequent air cooling yielded struvite, dittmarite, and newberyite in the solution with pH values of 9 and 10. By heating reactor at temperatures of 80 and 120 °C and water quenching, however, a pure dittmarite could be grown in the solution with any pH values (7–10). Dittmarite was also the major phase precipitated in the solution with any pH condition at 120 °C for the longer reaction time (96 h). A small impurity of sylvite was unexpectedly co-precipitated in all processes. SEM micrograph showed that the crystal solids have irregular prismatic-shaped morphology. The optimal pH for MAP crystallization was predicted to be about 9. The present results provided valuable information for the understanding of phosphate recovery from effluent by the hydrothermal treatment.

1. Introduction

Struvite [$\text{MgNH}_4\text{PO}_4 \cdot 6\text{H}_2\text{O}$] precipitation has gained much interest to provide an environmentally sound and renewable nutrient source from wastewater [1]. Nitrogen and phosphorus are frequently rich in wastewater and could be a potential source of struvite crystallization for the fertilizer industry, in case, that the nucleation and the quality of crystal product could be controlled by such a reactor technology [2]. Currently, precipitation technology through either calcium phosphate (CP) or magnesium ammonium phosphate (MAP) formation (i.e. struvite) has been developed for the recovery of ammonium and phosphate from wastewater effluents [2]. Nowadays, because of its low solubility, struvite can be precipitated as a commercial product for a slow-release fertilizer at high application rates. In the marketplace, a modified struvite crystal structure specifically diammonium phosphate (DAP) [$(\text{NH}_4)_2\text{HPO}_4$] and triple superphosphate (TSP) [$\text{Ca}(\text{H}_2\text{PO}_4)_2 \cdot 2\text{H}_2\text{O}$] [3], which has been treated with phosphoric acid, can be considered as a fertilizer with improved phosphorus release property. This modified struvite structure consists of two parts of the slowly-soluble phosphate; namely mono hydrogen magnesium phosphate (MgHPO_4), and highly

soluble DAP. This fertilizer product has potential to provide an initial high dose of phosphorus to the soil for a sustained slow-release of phosphorus.

Further, the induced MAP precipitation to yield struvite crystal relates to the process operation mode (i.e. batch, semi-batch or continuous) and crystallizer construction (e.g. fluidal bed, with internal suspension circulation), the intensity of mixing and/or circulation of solution or suspension, temperature, the chemical composition of wastewater. Principally, the struvite formation occurs through the following reaction (with $n = 0, 1$, and 2, as a function of pH) [2]:



Various mechanisms are possible for struvite crystallization depending on the supersaturation level in the crystallizer, whereas the supersaturation may be controlled by the content of ammonium, magnesium, and phosphate in an aqueous solution. However, the MAP precipitation is more sensitive to pH than the magnesium ion concentration added to the solution [4]. Moreover, the struvite precipitation from the aqueous solution could be manipulated by altering pH (6.5–11.5) [2,5], mixing energy [6], presence of foreign ions [7,8] and

* Corresponding author.

E-mail addresses: apbayuseno@gmail.com (A.P. Bayuseno), wolfgang.w.schmahl@lrz.uni-muenchen.de (W.W. Schmahl).

under dynamic temperature condition [9].

Because of its high P content (28.9% P_2O_5 or 9.8% P), struvite is potential as an ideal fertilizer, and the precipitation of struvite from wastewater has become an intensive research for the industrial fertilizer [3]. The use of struvite for fertilizers promotes lower leaching rates and extends discharge of nutrients during the growing season of plants [3]. Here, struvite with the granular form is preferred for the best slow release P fertilizers [3]. In particular, the hydrothermal method is an interesting technique to produce minerals in the granular form [4]. In this way, the hydrothermal parameters (i.e., temperature, force per unit area, and supersaturation of solution) could determine the yielding of struvite powder with homogeneous particle size.

Further struvite could be formed by inducing MAP precipitation under a hydrothermal condition which would provide as an economical and effective approach for phosphorus recovery, with high-quality crystallization products [4,10]. In this manner, a sewage sludge/water mix is usually put forward up to a sub-critical temperature (150–320 °C) and pressure (20–150 bar) in the presence of oxygen or nitrogen. The process may follow along two routes; (i) wet oxidation with oxygen available, or (ii) thermal hydrolysis in the presence of nitrogen [11]. Additionally, the hydrothermal treatment of wastewater can reduce the solids content substantially, whereas harmful heavy metals are concentrated them to smaller volume solid residue, which in turn yields in the release of nutrients (e.g., phosphate) from sewage sludge solids and other valuable by-products such as acetic acid and alcohols [4]. However, the benefits of the struvite crystallization under the hydrothermal condition has not been fully understood. Additionally, only a few studies have examined the hydrothermal precipitation of struvite-based phosphate recovery processes, which critically depends on a higher temperature and in excess water as well as cooling rates to room temperature. Here, a knowledge of the thermal stability of struvite and its possible phase transformation at a different hydrothermal temperature could help to ensure the purity and controlled morphology of struvite during crystallization.

Under dynamic temperature, struvite may decompose to dittmarite ($MgNH_4PO_4 \cdot H_2O$), which contains a higher P_2O_5 (45.7%) or P (19.9%) than that in struvite [9]. Moreover, the dittmarite formation could be benefits to extend the field of P recovery from wastewater. However, the economic analysis of this transformation is required for providing a cost-effective option in the phosphate recovery strategy. Conversely, the higher release of P_2O_5 to the soil is provided by struvite than that of dittmarite, because of greater dilution with water during crystallization. In addition, dittmarite gradually hydrate to be struvite as it contacts with soil moisture at ambient temperatures [9]. Therefore, thermal stability, phase transition and decomposition of the struvite system has been becoming a big concern on controlling struvite product in anaerobic digestion and post-digestion processes, as well as off-site, agricultural use.

Correspondingly, there is also a delicate equilibrium of struvite with other minerals in the aqueous solution resulting in other crystal phases [12]. In such case, magnesium phosphates such as $MgHPO_4 \cdot 3H_2O$ (newberyite), $Mg_3(PO_4)_2 \cdot 8H_2O$ (bobierrite) and $Mg_3(PO_4)_2 \cdot 22H_2O$ (cattiite) are frequently formed in addition to struvite crystallization [13,14]. A change of solid phases from newberyite to struvite or/to cattiite is also possible at an increasing pH from slightly acidic to slightly basic values. Nonetheless, both newberyite and struvite are commonly found thermodynamically stable at a pH range between 6.4 and 7.7, whereas stable phases of both struvite and bobierrite can be achieved at alkaline pH. Additionally, cattiite is stable in the air at room temperature and then become unstable in water. Thus, it may subsequently decompose to bobierrite [13].

The struvite growth has been widely investigated in various mother solutions, for example, in the solution of artificial urine or in artificial wastewater [2,5,9]. However, no report is found in the literature on crystallization of struvite and subsequent decomposition in the hydrothermal solution. Principally, the hydrothermal solution containing hot

waters with varying temperatures from 50 to 300 °C in which struvite and other phosphate-bearing minerals could be crystallized by supersaturation and inducing nucleation [4].

The present work was undertaken to examine crystallization of struvite and its phase transition from the aqueous media using a hydrothermal autoclave reactor. The induced MAP precipitation within the reactor containing the hydrothermal solution was examined at an initial pH, dynamic temperature condition and cooling method to room temperature. An effort to understand the struvite stability and its phase transition involved in the complex hydrothermal system requires a chemical equilibrium model and material characterization (qualitative and quantitative) and morphological analysis of the precipitating product. Here, the experimental material characterization of crystal growth, the phase change and morphological development from the hydrothermal synthesis were performed by XRPD (X-ray powder diffraction) and SEM analysis. These findings are expected to provide an approach in designing novel struvite based hydrothermal synthesis and the subsequent controlled homogeneous particle size.

2. Materials and methods

2.1. Crystal forming solution for hydrothermal synthesis

In the study, the crystal synthesis was performed by the hydrothermal method from an aqueous stock solution prepared by mixing an analytical grade powder of 0.025 M $NH_4H_2PO_4$ (VWR Chemicals) and $MgCl_2 \cdot 6H_2O$ (Fluka-Chemie) and subsequently diluted in distilled water to yield the stock solution with the equimolar ratio of MAP (1:1:1). The pH solution (7, 8, 9, and 10) was adjusted by dropwise addition of 50% w/w KOH (Merck) with stirring resulting in a white colloidal suspension. In this way, the stock solution was allowed to mix up in a time of reaction for 20 min at a low stirring rate (60 rpm) using a magnetic stirrer, while the pH solution was observed by digital control of the pH meter. The resulting precursor suspension was transferred to Teflon lined stainless steel autoclave of 50 ml capacity filled 80% with reaction media. Then the autoclave was heated in the furnace to a desired temperature (60, 80 and 120 °C) for 24 h, while an autogenous pressure was generated within the autoclave. After achieving required temperature and time for reaction, the autoclave was cooled through two-different routes to room temperature; (i) air cooling and (ii) quenching with water. Obtained precipitates were filtered by using filter papers (Wattman) and rinsed with distilled water several times to get rid of salt which was raised during the reaction. The obtained slurries were dried for at least 24 h just prior to conducting material characterization.

2.2. Saturation index calculation

The potential of minerals (e.g. struvite, newberyite and bobierrite) precipitated at particular hydrothermal conditions, were examined using a thermodynamic chemical equilibrium model of the AQION software program version 3.0. Calculations were conducted using the Davies activity coefficient approximation. The program was employed to calculate the saturation index (SI) using the input data of ion concentrations in the solution. The SI can be defined as:

$$SI = \log(IAP/K_{sp}) \quad (2)$$

where IAP refers to the ion activity product and K_{sp} is the solubility product of MAP. The unsaturated solution refers to $SI < 0$, and the precipitates may not be found. The spontaneous precipitation can occur in the saturated solution with $SI > 0$. The chemical composition of the synthetic wastewater for the input of the program is given in Table 1. The model of mineral species was subsequently calculated by the program, using pH values (7–10) and temperatures (60, 80 and 120 °C) as the input parameters.

Table 1

Concentration of reagents used for the hydrothermal synthesis.

Mg ²⁺ (g/l)	NH ₄ ⁺ (g/l)	PO ₄ ³⁻ (g/l)	Cl ⁻ (g/l)	K ⁺ (g/l)
0.6076	0.4509	2.374	1.7726	8.6993

2.3. Materials characterization

For the XRPD measurement, a standard technique has been developed for filling a capillary glass tube of 0.5 mm diameter with powder and the XRPD pattern was recorded by an STOE-diffractometer (Germany) in transmission (Debye-Scherrer) geometry using Mo-K α radiation ($\lambda = 0.70926$ Å) and generator of 50 kV/30 mA. The measured XRPD data were collected in a 2θ range between 3 and 50 and at step size 0.01°/step. Identification of crystalline substances was initially performed by MATCH software. The identified crystalline phases of the search match method were then verified by the Rietveld refinement method with Program X'Pert plus version 1.0 (Philip Analytical B.V). The crystal structure model for the Rietveld refinement was obtained from the literature (AMCSD-American mineralogist of crystal structure database). The refined cell parameters were then used for calculation of the weight. % levels of mineralogical phases, which was run by the program.

The dried precipitates were also characterized through SEM coupled with an energy dispersive X-ray analysis (SEM-EDX) and X-ray diffraction method. In this way, the powdered samples were initially placed on the Al-sample holder and then coated by carbon prior to conducting SEM characterization for morphology of the crystal phases.

3. Discussion and results

3.1. Mineral identification by XRPD and SEM analysis

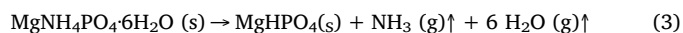
The dried precipitates obtained from the hydrothermal reaction time of 24 h at various pH, a temperature of 60 °C and followed by air cooling process were initially examined by XRPD search-match method to identify the mineral phases controlling the magnesium, ammonium, phosphate levels in the solution. The powdered XRPD patterns matched very well with the line data of struvite, and sylvite (KCl). Furthermore, those identified minerals were subsequently confirmed by the full profile XRPD Rietveld refinement. The diffraction peaks of assigned phases could be matched with the XRPD pattern of the AMCSD for struvite and sylvite, in which the difference plot of the calculated and the measured diffraction profile shows in close agreement. For the example of illustration, but the refinement result of precipitate at pH 8 and temperature of 60 °C is presented (Fig. 1a). As such, no significant amorphous phase was also seen in the precipitates as can be noticed in the background XRPD profile.

Fig. 1b shows the XRPD patterns of the dried precipitates at different pH and the temperature of 60 °C, which had been confirmed by the Rietveld method. The presence of struvite and sylvite is shown in the intensity profile corresponding to the AMCSD. The results show that the only peaks of struvite and sylvite were found in the pH range (7–10). The XRPD data were further analyzed by the quantitative Rietveld method and the results are given in Table 2. Results confirmed that the purity in the range of 98–100 wt.% for struvite was produced in all precipitates, while a minute of sylvite (0.2–1.1 wt.%) was frequently found. The impurity formed is probably corresponding to the drying process of the precipitates.

The SEM images of struvite morphology synthesized at different pH, the temperature of 60 °C and the reaction time of 24 h with air cooled are shown in Fig. 2. Irregular prismatic-like struvite was obtained with an average diameter of 40 μ m when the synthesis was performed at initial pH 7. When the pH reaction was increased to 8, the morphology remained intact, but an average particle shows increasing in size

(Fig. 2b). These prismatic-like structures consisted of numerous nanoplates. More specifically, struvite crystal precipitated under influence of the low temperature (60 °C) and pH (7–8) was less well-formed and without distinct morphology. Conversely, when the pH solution was further increased to 9, the prism-like structures changed in prismatic shape, but with a slightly smaller crystalline (Fig. 2c). Later, this structure remained stable, as pH increased to 10.

A similar hydrothermal synthesis was performed by adjusting the initial pH (7–10), while the reaction time of 24 h, the temperature 80 °C and subsequently air-cooled to room temperature was selected. The mineral compositions of these four samples were then identified by the XRPD Rietveld method. As shown in Fig. 3, some peaks in the XRPD patterns could be assigned to AMCSD corresponding to dittmarite, newberyite, struvite, and sylvite. It is noticeable in Table 2 that struvite was the major phase in the sample obtained in the pH range of 7–8 and the temperature of 80 °C. However, at the same condition, the presence of dittmarite and newberyite were observed at pH of 9 and 10. The reason for the absence of newberyite in the pH 7 and 8 could be related to the concentration of magnesium ions and pH of the system [15]. In general, newberyite could be formed as a product of decomposition of struvite or directly precipitated in association with struvite. Conversely, dittmarite may be formed from the dissolution of struvite, of which the concentration of hydrogen ions controls the reaction between the ionic species [9]. In this case, the solution with a pH of 7 and 8 was proposed to be still rich in ammonia and magnesium, which is favorable for dittmarite formation rather than newberyite. Thus decomposition products for samples, which were heated from 60 to 80 °C, contained a mixture of phases as a result of the evolution of H₂O (g) upon heating and subsequent air cooling. The formation of dittmarite and/or newberyite may correspond to the reaction of mass loss below [9]:



Under the hydrothermal reaction, however, H₂O(g) and NH₃(g) remained in the autoclave reactor upon heating and air cooling, which subsequently contributed to struvite decomposition. Normally, struvite decomposition into dittmarite in the air may occur below 125 °C [9,16].

In the results of struvite transformation at the temperature of 80 °C, the presence of dittmarite, and newberyite were noticed at pH of 9 and 10. From pH 7 to 10, a drop content of struvite was observed until its content remained approximately 15.8 wt.%. As a consequence of increasing initial pH, the amount of dittmarite increased, suggesting a decomposition of the struvite product to dittmarite assisted by the pH solution and air cooling of the hydrothermal reactor. It has been reported previously that a product of struvite transformation in the presence of excess water, could be contributed by the loss of ammonium and water at the increasing temperatures (> 55 °C) [9]. At the temperature of 80 °C, heating of the mixtures in the sealed conditions resulted in most of the ammonia, if not all, being transformed into NH₃ species. The simultaneous release of both NH₃ and H₂O molecules corresponded to the formation of dittmarite and newberyite, in which struvite could have decomposed in the solution with the pH of 9 and 10. They would subsequently be found as the crystal product after air cooling. Here, newberyite was found in the sample, perhaps related to the struvite decomposition during the slow air cooling of the reactor. The observations of this study are also confirmed by some previous findings according to which struvite can have decomposed to newberyite at room temperature of 20 °C [17,18]. Furthermore, the finding of the small amount of sylvite was related to the drying process of the slurries.

The SEM images of as-hydrothermal synthesized samples obtained at the various pH and the defined reaction time and temperature (24 h, and 80 °C) are shown in Fig. 4. At the pH of 7–8, the crystals obtained showed an aggregate formation of plate-like crystallite on top of the surface of the larger struvite crystals (Fig. 4a and b). When pH was increased to 9, a prism-like structure was obtained with a small particle

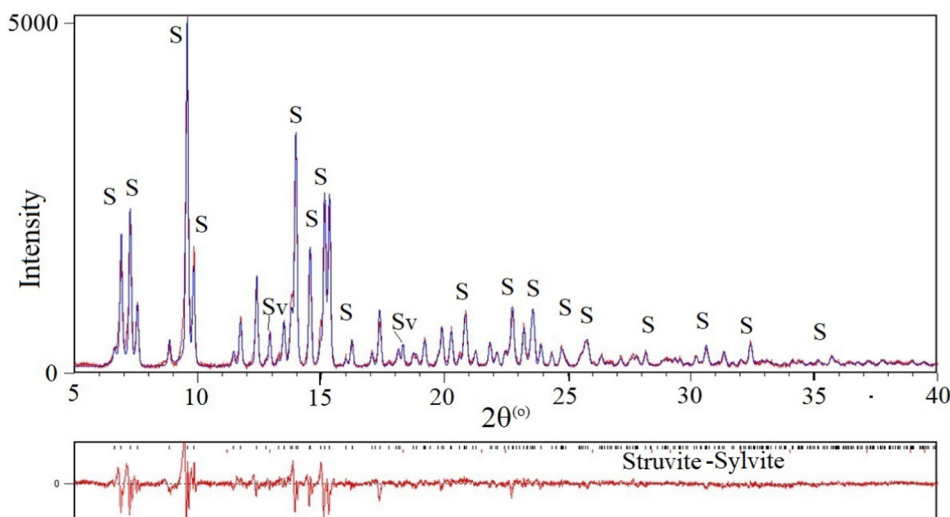


Fig. 1a. XRPD Rietveld plot of crystallized product obtained from the hydrothermal reaction at pH 8, temperature of 60 °C, time = 24 h and air-cooled to room temperature. Note: S = struvite, Sv = sylvite.

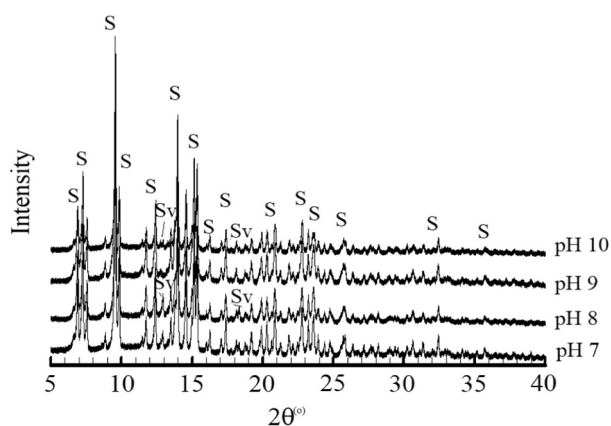


Fig. 1b. XRPD pattern of crystallized product obtained from the hydrothermal reaction at various pH, temperature of 60 °C, time = 24 h and air-cooled to room temperature. Note: S = struvite, Sv = sylvite.

Table 2

Phase composition of the solid precipitated from the hydrothermal reaction and subsequent air cooling to room temperature.

Temperature/time	Mineral	Initial pH solution			
		7	8	9	10
		Wt. %			
60 °C/24 h	Struvite	98.9	98.9	99.8	99.5
	Sylvite	1.1	1.1	0.2	0.5
80 °C/24 h	Dittmarite	35.1	41.1	69.3	73.9
	Newberyite			19.4	9.9
	Struvite	63.6	58.4	10.4	15.8
	Sylvite	1.3	0.5	0.9	0.4
120 °C/24 h	Dittmarite	3.9	6.3	5.6	12.5
	Struvite	95.7	91.3	91.7	86.4
	Sylvite	0.4	2.4	2.7	1.1

distribution (Fig. 4c). However, the hydrothermal synthesis performed at pH 10, the aggregate formation of small-and large prismatic crystallite was observed in Fig. 4d. Such aggregate generated during the decomposition process indicates both dendritic crystals of struvite and small crystals of newberyite, which is the similar to finding of work by Babic-Ivancic et al. [17,18].

In the case of hydrothermal synthesis at the temperature of 120 °C and the various pH (7–10) with air-cooled, dittmarite was the only decomposition product of struvite confirmed by the XRPD Rietveld method (Fig. 5 and Table 2). However, dittmarite was not the major phase found in the samples, and the amount of dittmarite was insignificantly affected by the increase in pH from 7 to 10. This indicated no further change of phase composition in the sample. Conversely, the further increase in temperature led to the decreased formation of struvite, but it was nonetheless the major form in the samples in addition to the impurity formation of sylvite. With the hydrothermal condition at 120 °C, the orthophosphate activity appeared also increasing in the excess water, implying that dittmarite other than struvite was present [19]. Subsequently, dittmarite was slowly hydrated in the solution during air cooling, but not all being transformed to struvite in the course time of reaction. As discussed in the next section, however, dittmarite hydration could not be observed in the precipitate during the water quenching. This shorter time duration may not allow dittmarite to transform to struvite.

Furthermore, a prism-like structure with a larger size distribution (> 100 μm) was observed by SEM on the sample obtained from the pH of 7 and the temperature of 120 °C (Fig. 6a). When pH was further increased to 8–10, the reduction of crystal size was detected, and also the distribution seems to be relatively more equal at pH of 9 and 10. In this way, the hydrothermal temperature of 120 °C was proposed to influence significantly the crystal growth of struvite [9].

3.2. The effect of water quenching on the mineral formation

The precipitates were investigated over a wide range of initial pH after various heating temperatures for 24 h and water quenching to room temperature. Fig. 7 shows the XRPD diffractogram of the solid crystals obtained by hydrothermal synthesis and water quenching. Obviously, struvite was precipitated in the whole pH range and temperature of 60 °C observed in the present study. The hydrothermal experiments performed under the influences of temperatures (80 and 120 °C) showed the appearance of dittmarite. Detailed XRPD quantitative analyses were also performed on the precipitate formed (Table 3). The analyses of the crystal solid obtained after heating the reactor system at the temperature of 60 °C for 24 h and subsequently water quenching provided that struvite is a major crystalline phase. By increasing temperature (80 and 120 °C) at varying initial pH, and following water quenching, however, the content of dittmarite in all precipitates increased to almost 99 wt.%. It is obvious that the

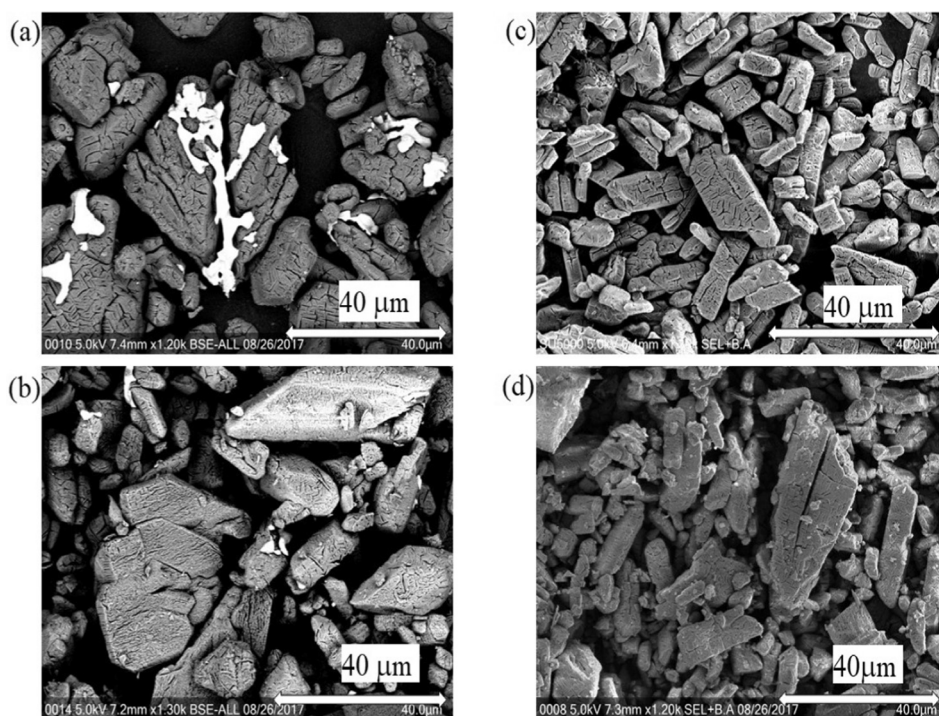


Fig. 2. SEM micrographs of crystallized product obtained from the hydrothermal reaction at various pH (7, 8, 9, 10), temperature of 60 °C, time = 24 h and air-cooled to room temperature.

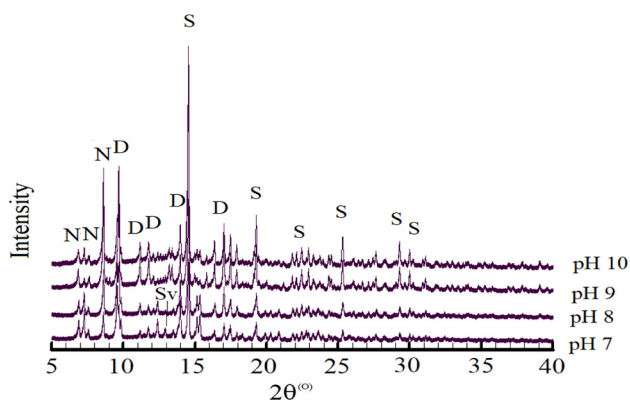


Fig. 3. XRPD pattern of crystallized product obtained from the hydrothermal reaction at various pH, temperature of 80 °C, time = 24 h and air-cooled to room temperature. Note: D = dittmarite, N = newberyite, S = struvite and Sv = sylvite.

temperature of 60 °C is the favorable conditions for hydrothermal synthesis of pure struvite, which could be established indifference to the initial pH selected [9]. Thus, the increase in temperature of the reactor system (from 80 to 120 °C), lead to struvite to transform into dittmarite soon afterward. The possible transformation mechanisms of various phases associated with struvite precipitation have been previously reported by Bhuiyan et al. [9] and suggested that struvite decomposition depended on both supersaturation and ammonia activity in the solution. When the reactor was heated from temperatures of 80–120 °C, some ammonia and water molecules were simultaneously released. At these temperatures, struvite was entirely transformed into dittmarite, but it was slowly hydrated in the hydrothermal solution during air cooling, where the resulting hydration product was struvite at room temperature. Conversely, the quenching method of the reactor did not allow dittmarite to return to struvite in the short time duration of the reaction. Moreover, the subsequently dropped temperature in the system by water quenching made a crystal growth of dittmarite being

now the only process. Finally, dittmarite in this system remained stable at room temperature.

3.3. The effect of the pH solution on mineral formation

The pH solution plays a vital role in determining the ion speciation and the SI of the mineralogical phase [9]. The effect of pH value on SI values of different mineral phosphates under hydrothermal reaction system was designed with MAP concentration at 25 mM in which the substance concentration ratio of Mg: NH₄: PO₄ = 1:1:1 while maintaining ionic strength with 0.01 mM KNO₃. The calculated results of corresponding SI values for all minerals possible found as a function of pH solution are shown in Fig. 8. In this work, dittmarite was not entered into the AQION model because its solubility product was not available in the literature.

At the temperature of 60 °C, the SI value of struvite remained constant at 0 when the solution pH value increased (Fig. 8a). The similar variation trend is shown in SI value of newberyite in the pH range of 7–8. However, once the pH value gradually increased from 8.0 to 10, the SI values of newberyite reduced accordingly. In this way, bobierrite grew gradually, reaching the peak when the pH value reached 9.0, and then reduced as the pH value increased.

It is noticed that there are optimum pH values for crystallization of bobierrite and brucite, with an optimum pH value be around 9–10 for both minerals. Within the scope of optimum pH value, the SI values turn on to be SI brucite < SI bobierrite. It should bear in mind that the AQION software program did not account for the kinetics of the possible mineral precipitation. In the present study, struvite would presumably precipitate in a short reactor residence time, whereas bobierrite would precipitate in the order of days or months [20,21]. Therefore, it was proposed that the slow-forming minerals (e.g., bobierrite) with having SI positive value might be not identified in the subsequent XRPD analysis.

A similar calculation of SI of the solution was carried out by adjusting the temperature of 80 °C. Fig. 8b presents the impact of solution pH value on the SI values of magnesium phosphate salts. The

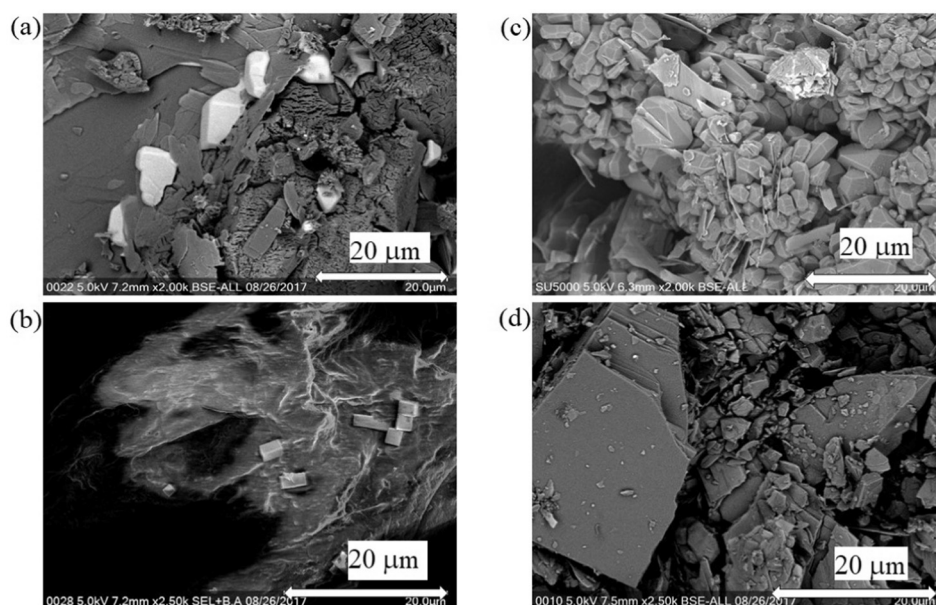


Fig. 4. SEM micrographs of crystallized product obtained from the hydrothermal reaction at various pH (a–d) (7, 8, 9, 10), temperature of 80 °C, time = 24 h and air cooled to room temperature.

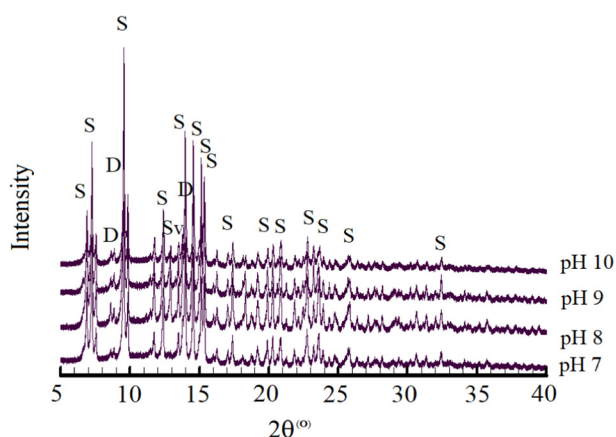


Fig. 5. XRPD pattern of crystallized product obtained from the hydrothermal reaction at various pH (a–d) (7, 8, 9, 10), temperature of 120 °C, time = 24 h and air-cooled to room temperature. Note: D = dittmarite, S = struvite and Sv = sylvite.

crystallization of struvite and newberyite is under equilibrium with $SI = 0$ at pH 7 and tends to be under saturation when pH value increased from 8 to 10. In contrast, bobierrite grew gradually under supersaturated solution, reaching the peak at pH 8. However, struvite and newberyite could precipitate simultaneously and coexist under certain pH conditions [9]. With the pH value ranging from 8 to 10, the magnitude of SI for newberyite and bobierrite was changed. In this case of increasing pH, the SI value of newberyite decreased, while the SI value of bobierrite decreased accordingly. Additionally, SI values of brucite increased gradually with the increase of pH, though increasing, the magnitude of change for increasing SI was slightly increased. Under the hydrothermal reaction temperature of 80 °C, cattite, bischofite, and sylvite kept undersaturated condition with the increase in pH value. The similar trends in SI values for all minerals with varying pH were obtained in the calculation by adjusting the temperature to 120 °C (Fig. 8c). In this case, struvite crystallized under equilibrium solution with $SI = 0$. The SI value of bobierrite reaches the peak at pH 8. From the modeling thermodynamic simulation results, the adjustment of initial pH value is the important method to control the precipitation

reaction of struvite during phosphate recovery. The pH value in the hydrothermal synthesis should be adjusted to be within 8–9. Model simulations showed that increasing pH to 8 and 9 with the induced magnesium into the hydrothermal solution made the reduction in the soluble phosphorus. In this case, the pH 8 and 9 of the hydrothermal solution at any temperature (60, 80, and 120 °C) were estimated for the condition with the highest reduction in the orthophosphate (OP) concentration. Moreover, the significant ammonia losses were also shown with increasing pH (8 and 9). Based on the observed MAP ion reduction, it is more likely that a high amount MAP compound could be formed as struvite or dittmarite in the solution within the pH of 8 and 9.

To explore the impact of the solution pH value on the MAP precipitation was examined using the speciation of phosphate, magnesium, and ammonium ions in the solution. The products of the concentrations of Mg^{2+} , NH_4^+ , and PO_4^{3-} at different pH levels were simulated and the results are given in Fig. 9. It is also shown that the optimum pH value for crystallization of MAP minerals could be integrated with the changing reactive ion concentrations. With the pH value ranging from 7 to 9 and the temperature of 60 °C, the Mg^{2+} and PO_4^{3-} declined slightly (Fig. 9a). This was likely due to the increased activity of Mg^{2+} and PO_4^{3-} in the solution, possibly yielding in the development of struvite formation. With the increase in pH from 8 to 10, the reaction products of NH_4^+ and PO_4^{3-} was not so high, while the Mg^{2+} concentration reduced gradually. The results suggest that there was a minimum of the MAP crystallization product at a pH close to 9. With the increased pH from 10, the reactive ammonium and phosphate decreased, which may be due to the solubility of struvite. The further increase in pH may yield in the increased free ammonia and ammonia gas fractions, also the crystallization of Mg complexes such as $(MgOH)^+$, and the precipitation of Mg salts, such as brucite $Mg(OH)_2$, i.e. reduction in activities of Mg^{2+} and NH_4^+ . The results may also indicate that a minimal thermodynamic solubility product of struvite could be achieved at a pH within 9 and 10, while reasonably agreed with the reported prediction of a minimum solubility of struvite in the pH ranging from 8.9 to 9.3 under fresh water conditions [22,23]. The little difference of the present result could be related to the disparity of ionic strength employed in the calculation.

Across the pH range (7–10) and temperature (60, 80 and 120 °C) and time (24 h) examined, the model predicted Mg^{2+} and PO_4^{3-} to be most reactive ions, followed by NH_4^+ (Fig. 9b and c). Depending on pH

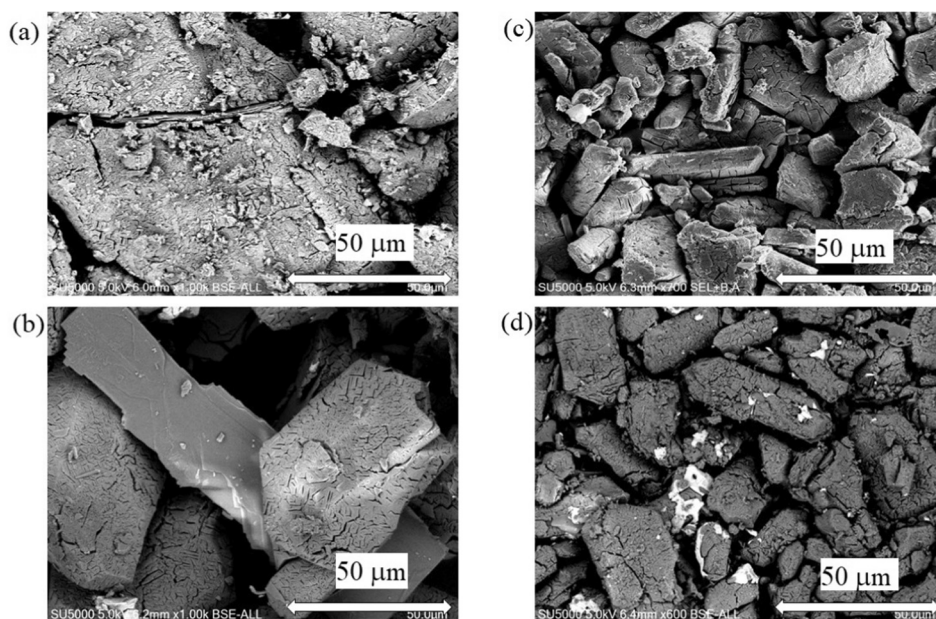


Fig. 6. SEM micrographs of crystallized product obtained from the hydrothermal reaction at various pH (a–d) (7, 8, 9, 10), temperature of 120 °C, time = 24 h and air-cooled to room temperature.

and temperature, the NH_4^+ and PO_4^{3-} concentrations increased gradually, making the SI values of ammonium, magnesium and phosphate ions decreased gradually. It is proposed in the present study, the appropriate pH value should be controlled to be between 8.0 and 9.0 under hydrothermal reaction.

3.4. The finding of study by hydrothermal method

The thermodynamic modeling of MAP precipitation in the hydrothermal experiments on various pH value and temperatures has been verified, providing that the experimental results were in close agreement with the predictions of the thermodynamic model except for pH of 9 and 10 at the temperature of 80 °C. Although newberyite was modeled to be undersaturated with struvite, it was identified by XRPD method. This is because the gradual loss of ammonium during heating made a low activity of ammonium in the solution, of which struvite became a metastable phase and was likely to transform to newberyite [24]. Established along the model of OP reduction in the solution, the optimum pH range for MAP precipitation was 8–9. However, the XRPD analysis verified that the cooling method has significantly influenced on the struvite decomposition rather than the pH control.

Further, at temperatures of 80 and 120 °C, dittmarite was the major phase under both of air cooling and water quenching (Tables 2 and 3), though it was not modeled in the AQION program. Here, dittmarite was not introduced into the thermodynamic model, but it was found in the XRPD analysis because once dittmarite was introduced into the excess water, it could rehydrate to struvite before dissolution and therefore would follow struvite solubility closely [9,25]. The experimental results were in qualitative agreement with the correlation of the SI for the MAP precipitation. The phosphate recovery decreased with the increase in pH and temperature observed during the study. The optimum magnesium, ammonium and phosphate recovery for MAP precipitation was reached at pH 8 and temperature of 80 °C. However, the excessive Mg reduction was not effective for additional ammonium and phosphate removal and recovery of high pH value (9–10).

However, the XRPD analysis revealed that the hydrothermal synthesis with different temperatures and pH provided a mixture of struvite, newberyite, and dittmarite. With two different cooling methods in the reactor examined, either pure struvite or dittmarite could be synthesized from the temperature investigated (Fig. 10). The

cooling mode of the hydrothermal reactor has a substantial role in the performances of struvite production. A literature review had been carried on each of the phosphate minerals to determine the likelihood of formation in a period of time and subsequent mineral stabilities achieved after cooling of the reactor [9,24]. It has been demonstrated that struvite, newberyite, and dittmarite can be precipitated in the short period of time, while bobierrite and cattite could be formed at longer time duration of the reaction. With the chemical equilibrium model in the AQION program, the precipitation of those minerals is possible. Despite the possibility of struvite formation in the different condition, the model could predict its formation more successfully for an increasing pH and temperatures. However, the precipitation kinetics of all minerals were not counted in the AQION program. Therefore, the model simulations provided underprediction for the potential of bobierrite precipitated in the hydrothermal solution as can be seen in Fig. 8a–c.

Furthermore, the loss of water and ammonium at the increasing temperature and pH in the sealed condition are important factors for struvite decomposition, while the cooling method may contribute to the rehydration of struvite structure [26]. It was shown that the general trend of struvite formation or its phase decomposition during cooling is signified by an arrow. Presumably, the transformation of dittmarite to struvite could have resulted from the slow hydration in the solution. Here struvite was the major phase obtained from the air cooling. With the quenching method, however, the major phase obtained was dittmarite. The hydrothermal behavior of struvite reported in the study has important implications for engineering operations. By precipitating struvite or dittmarite under hydrothermal reaction, the nutrient such as P and N can be recovered from the wastewater that may lower high production costs compared to other precipitation technology [27]. However, any bobierrite and cattite were not identified in XRPD analysis. This was probably bobierrite and cattite, which were reported to have a low precipitation rate in the order of days or months [20,21].

Further, this hypothesis for the lower precipitation rate of bobierrite may be supported by the experimental evidence of hydrothermal synthesis for longer reaction time. The present outcome of the hydrothermal synthesis for a long time (96 h) at the temperature of 120 °C and subsequent air cooling showed that the more stable octahydrate, bobierrite did not grow, while dittmarite was the major crystalline phase obtained in the solution with any pH condition (Fig. 11; Table 4).

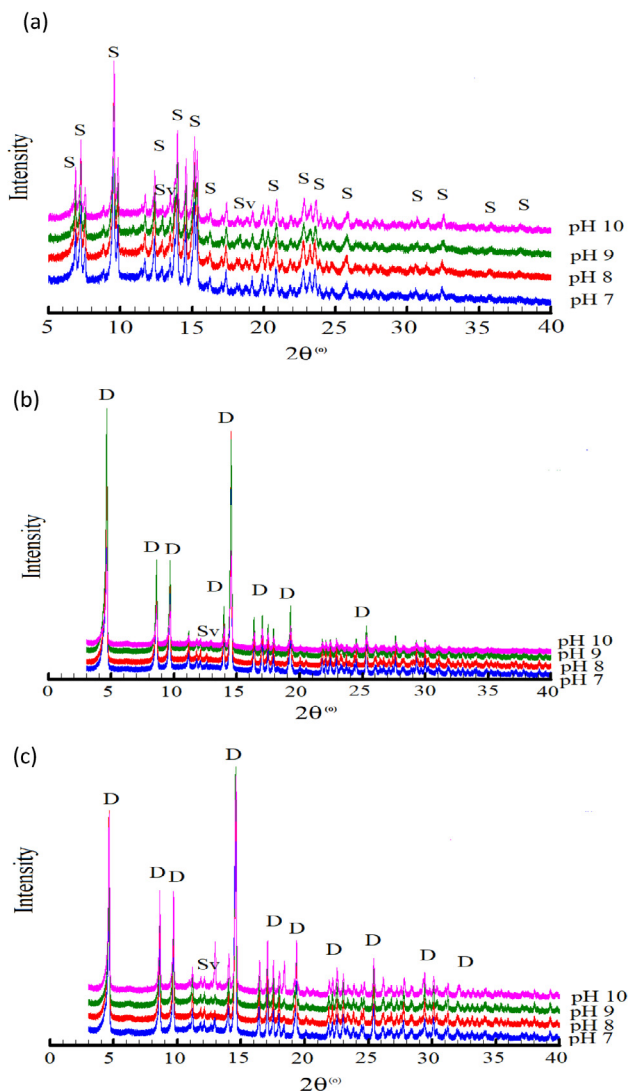


Fig. 7. XRPD pattern of crystalline product obtained from the hydrothermal reaction at various pH (7, 8, 9, 10), and temperatures of (a) 60; (b) 80 and (c) 120 °C, time = 24 h and water-quenched to room temperature. Note: D = dittmarite, S = struvite and Sv = sylvite.

Table 3

Phase composition of the solid precipitated from the hydrothermal reaction and subsequent water quenching to room temperature.

Temperature/time	Mineral	Initial pH solution			
		7	8	9	10
		Wt. %			
60 °C/24 h	Struvite	98.6	99.1	98.3	99.5
	Sylvite	1.4	0.9	1.7	0.5
80 °C/24 h	Dittmarite	99.5	99.8	99.7	99.3
	Sylvite	0.5	0.2	0.3	0.7
120 °C/24 h	Dittmarite	98.5	98.8	99.1	94.8
	Sylvite	1.5	1.2	0.9	5.2

In the solution with a pH of 7, struvite was partially transformed to dittmarite. However, with the increasing pH (8–10) at this temperature, struvite was totally replaced by dittmarite during heating. Obviously, the longer reaction time at high temperature (> 100 °C) has the significant effect on the change of struvite structure, in which there was a loss of five water molecules leading to struvite decomposition to

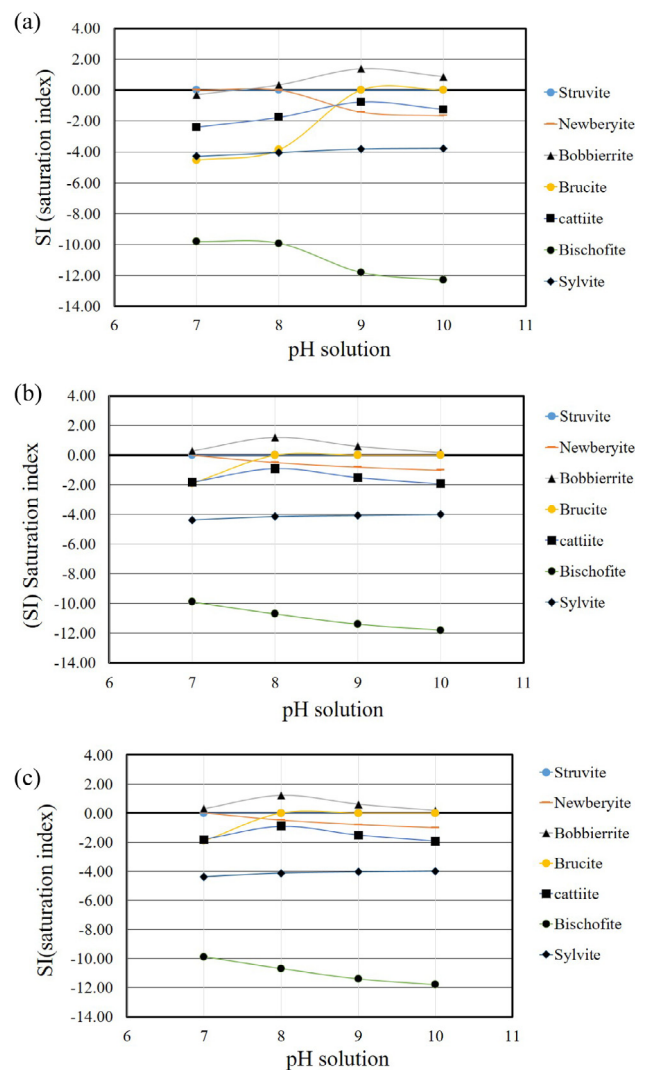


Fig. 8. The effect of solution pH on the SI value of the precipitation system with different temperature (a) 60; (b) 80 and (c) 120 °C.

dittmarite [9]. Subsequently, dittmarite was likely to be the more stable phase during long time heating, thereby, in turn, remains stable during air cooling. Further research should be done in the synthesis of bobbierite with varying temperatures and pH of the hydrothermal solution for the longer reaction time. This term may allow struvite to transform to bobbierite at the certain hydrothermal condition.

In the SEM examination, the regular prismatic-like crystals were observed with the crystal length of about 100 μm, when the MAP molar ratio in the solution with any pH and temperatures was set-up to be 1:1:1, and their concentrations were 25 mM. The SEM image shows that the morphology of crystals could be identified through the surface of crystals was not smooth, being covered with other predicates. It is likewise shown that hydrothermal synthesis under the low temperature of 60 °C and basic pH value (8–9) has provided a strategy in the increased purity of struvite with the prismatic morphology.

4. Conclusion

It can be concluded that the use of the hydrothermal method in the solution, which was set up 1:1:1 at the equal concentration of 25 mM and followed by air cooling and water quenching, could explore the thermal behavior of struvite. The XRPD Rietveld analysis confirmed that the precipitates contained the phase abundance of struvite and/or dittmarite with the impurity of sylvite when the synthesis was

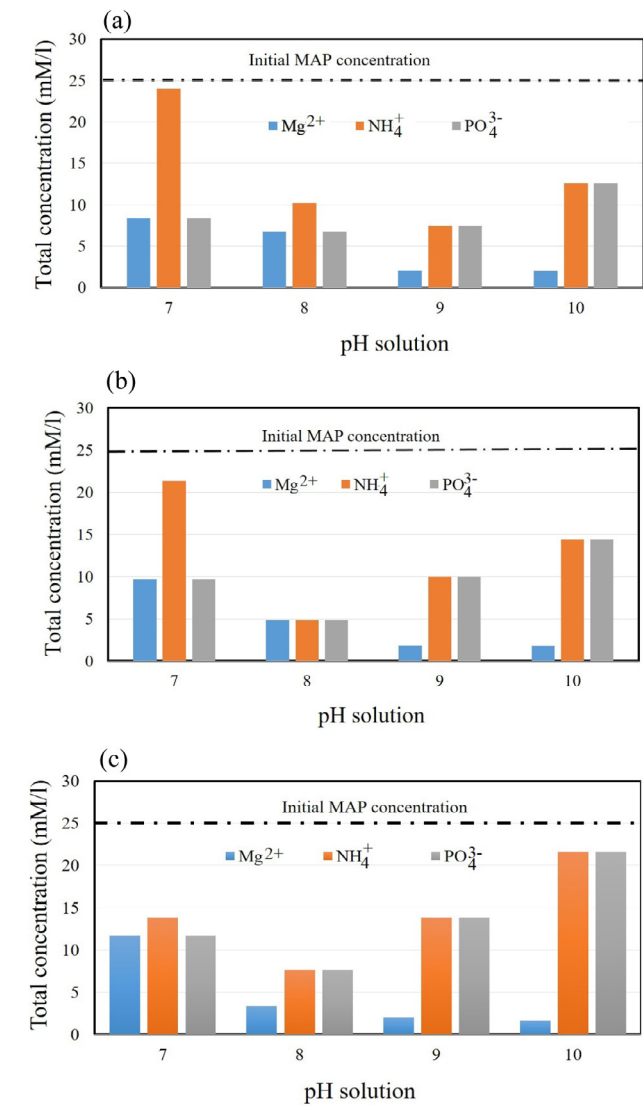


Fig. 9. The concentration of MAP (Mg^{2+} , NH_4^+ and PO_4^{3-}) ions in the super-saturated solutions as a function of pH and temperature of (a) 60; (b) 80 and (c) 120 °C.

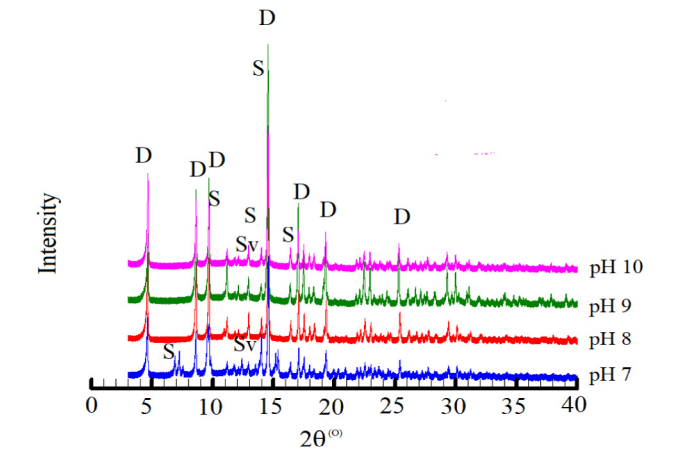


Fig. 11. XRPD pattern of crystallized product obtained from the hydrothermal reaction at various pH (7, 8, 9, 10), temperature of 120 °C, time = 96 h and air-cooled to room temperature. Note: D = dittmarite, S = struvite and Sv = sylvite.

Table 4
Phase composition of the solid precipitated from the hydrothermal reaction at temperature 120 °C, for 96 h and subsequent air cooling to room temperature.

Mineral	Initial pH solution			
	7	8	9	10
	Wt. %			
Dittmarite	55.6	95.1	96.7	94.2
Struvite	43.1			
Sylvite	1.3	4.9	3.3	5.8

performed at temperatures from 60 to 120 °C and followed by water quenching. Newberyite and dittmarite were frequently precipitated under the hydrothermal temperature of 80 °C with varying pH solution (9–10) and subsequent air cooling to room temperature. Upon various pH values (7–10), the SI values of struvite remained constant with the increase in temperature, while newberyite decreased with the increment in temperature at pH 9. The possible formation of struvite as a function of pH and temperatures was in agreement with the predictions of thermodynamic modeling, except for the prediction of newberyite formed in the solution with the pH of 9 and 10 at the temperature of

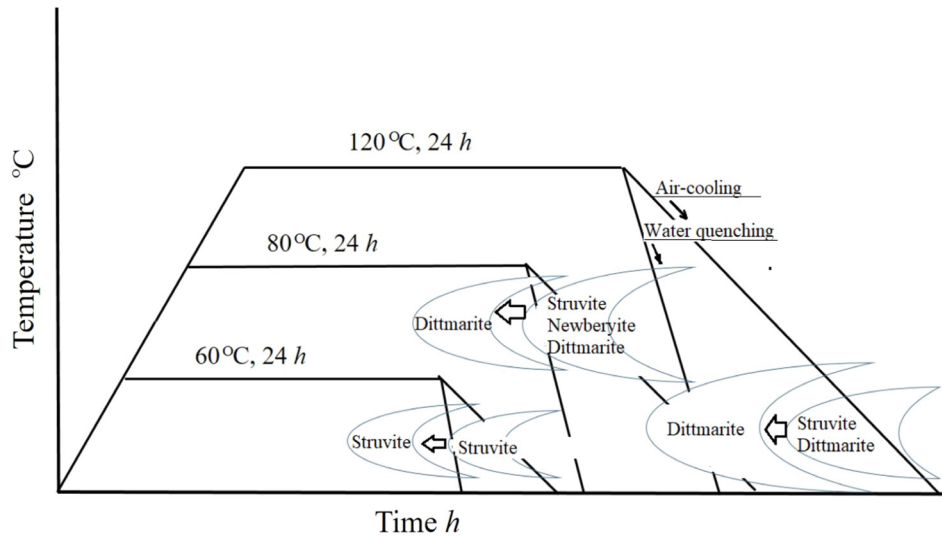


Fig. 10. Summary of an overall transformation process from hydrothermal condition and subsequent cooling method.

80 °C. The SEM images of crystals showed that the prism-like morphology was developed during the synthesis. In the case study of the hydrothermal method for phosphate recovery, temperature and subsequent cooling method were the main parameters influencing the phosphate-bearing mineral formation. The results of this study provided the valuable data that can be used for precipitation of struvite and other phosphate-bearing minerals in the hydrothermal system.

Acknowledgments

The study was supported by the KAAD (*Katholischer Akademischer Austausch Dienst*) Bonn, Germany for a sabbatical on leave study program at LMU Munich. The authors would like to thank Dr. Erika Griesshaber for her assistance in collecting electron microscope analysis data. The assistance of Stefanie Hoser performing laboratory experiments is also gratefully acknowledged.

References

- [1] J.D. Doyle, K. Oldring, J. Churchley, C. Price, S.A. Parsons, Chemical control of struvite precipitation, *J. Environ. Eng. -ASCE* 129 (2003) 419–426.
- [2] J.D. Doyle, S.A. Parsons, Struvite formation, control and recovery, *Water Res.* 36 (2002) 3925–3940.
- [3] M.R. Gaterell, R. Gay, R. Wilson, R.J. Gochin, J.N. Lester, An economic and environmental evaluation of the opportunities for substituting phosphorus recovered from wastewater treatment works in existing UK fertilizer markets, *Environ. Technol.* 21 (2000) 1067–1084.
- [4] M.T. Munir, B. Li, I. Boiarkina, S. Baroutian, W. Yu, B.R. Young, Phosphate recovery from hydrothermally treated sewage sludge using struvite precipitation, *Bioresour. Technol.* 239 (2017) 171–179.
- [5] N.C. Bouropoulos, P.G. Koutsoukos, Spontaneous precipitation of struvite from aqueous solutions, *J. Cryst. Growth* 213 (2000) 381–388.
- [6] K.N. Ohlinger, T.M. Young, E.D. Schroeder, Postdigestion struvite precipitation using a fluidized bed reactor, *J. Environ. Eng.* 126 (2000) 361–368.
- [7] K.S. Le Corre, E. Valsami-Jones, P. Hobbs, S.A. Parsons, Impact of calcium on struvite crystal size, shape and purity, *J. Cryst. Growth* 283 (2005) 514–522.
- [8] D.S. Perwitasari, L. Edahwati, S. Sutiyono, S. Muryanto, J. Jamari, A.P. Bayuseno, Phosphate recovery through struvite-family crystals precipitated in the presence of citric acid: mineralogical phase and morphology evaluation, *Environ. Technol.* 38 (2017) 2844–2855.
- [9] M.I.H. Bhuiyan, D.S. Mavinic, F.A. Koch, Thermal decomposition of struvite and its phase transition, *Chemosphere* 70 (2008) 1347–1356.
- [10] C. Sartorius, J. von Horn, F. Tettenborn, Phosphorus recovery from wastewater—state-of-the-art and future potential, *Proc. Water Environ. Fed.* 2011 (2011) 299–316.
- [11] K. Hii, S. Baroutian, R. Parthasarathy, D.J. Gapes, N. Eshtiaghi, A review of wet air oxidation and thermal hydrolysis technologies in sludge treatment, *Bioresour. Technol.* 155 (2014) 289–299.
- [12] A. Andrade, R.D. Schuiling, The chemistry of struvite crystallization, *Miner. J. Ukr.* 23 (2001) 37–46.
- [13] M.I.H. Bhuiyan, D.S. Mavinic, R.D. Beckie, A solubility and thermodynamic study of struvite, *Environ. Technol.* 28 (2007) 1015–1026.
- [14] T. Michalowski, A. Pietrzyk, A thermodynamic study of struvite in water system, *Talanta* 68 (2006) 594–601.
- [15] V. Babic-Ivancic, J. Kontrec, L. Brecevic, Formation and transformation of struvite and newberyite in aqueous solutions under conditions similar to physiological, *Urol Res.* 32 (2004) 350–356.
- [16] M.V. Ramlogan, A.A. Rouff, An investigation of the thermal behavior of magnesium ammonium phosphate hexahydrate, *J. Therm. Anal. Calorim.* 123 (2016) 145–152.
- [17] V. Babic-Ivancic, J. Kontrec, L. Brecevic, D. Kralj, Kinetics of struvite newberyite transformation in the precipitation system $\text{MgCl}_2\text{-NH}_4\text{H}_2\text{PO}_4\text{-NaOH-H}_2\text{O}$, *Water Res.* 40 (2006) 3447–3455.
- [18] V. Babic-Ivancic, J. Kontrec, D.K. Kralj, L. Brecevic, Precipitation diagram of struvite and dissolution kinetics of different struvite morphologies, *Croat. Chem. Acta* 75 (2002) 89–106.
- [19] W. Stum, J.J. Morgan, *Aquatic Chemistry*, Wiley-Interscience, New York, NY, 1970, p. 583.
- [20] I. Celen, J.R. Buchanan, R.T. Burns, R.B. Robinson, D.R. Raman, Using a chemical equilibrium model to predict amendments required to precipitate phosphorus as struvite in liquid swine manure, *Water Res.* 41 (2007) 1689–1696.
- [21] A.W. Frazier, J.R. Lehr, J.P. Smith, The magnesium phosphates hennayite, schertelite and bobierite, *Am. Mineral.* 4E (1963).
- [22] N.O. Nelson, R.L. Mikkelsen, D.L. Hesterberg, Struvite precipitation in anaerobic swine lagoon liquid: effect of pH and Mg: P ratio and determination of rate constant, *Bioresour. Technol.* 89 (2003) 229–236.
- [23] Y. Song, F. Qian, Y. Gao, X. Huang, J. Wu, H. Yu, PHREEQC program-based simulation of magnesium phosphates crystallization for phosphorus recovery, *Environ. Earth Sci.* 73 (2015) 5075–5084.
- [24] J. Kontrec, V. Babic-Ivancic, L. Brecevic, Formation and morphology of struvite and newberyite in aqueous solutions at 25 and 37 °C, *Coll. Antropol.* 29 (2005) 289–294.
- [25] J.D. Doyle, K. Oldring, J. Churchley, S.A. Parsons, Struvite formation and the fouling propensity of different materials, *Water Res.* 36 (2002) 3971–3978.
- [26] F. Montes, C.A. Rotz, H. Chaoui, Process modeling of ammonia volatilization from ammonium solution and manure surfaces: a review with recommended models, *Trans. ASABE* 52 (2009) 1707–1719.
- [27] N. Marti, A. Bouzas, A. Seco, J. Ferrer, Struvite precipitation assessment in anaerobic digestion processes, *Chem. Eng. J.* 141 (2008) 67–74.